Vol. 47: 191–208, 2007 | AQUATIC MICROBIAL ECOLOGY
Aquat Microb Ecol | Published May 16

Phytoplankton dynamics during an *in situ* iron enrichment experiment (EisenEx) in the Southern Ocean: a comparative study of field and bottle incubation measurements

Marcel J. W. Veldhuis*, Klaas R. Timmermans

Netherlands Institute for Sea Research, PO Box 59, 1790 AB, Den Burg, Texel, The Netherlands

ABSTRACT: Composition, physiology and growth response of 5 size classes of phytoplankton, ranging from 0.7 to 20 µm, was studied in an *in situ* iron enrichment experiment (EisenEx) and in bottle incubations in the Southern Ocean during austral spring 2000. In the field, iron enrichment resulted in only minor changes in numerical abundance, cell carbon content, photosynthetic efficiency (F_v:F_m) and the percentage of live cells of *Synechococcus* spp. and pico-eukaryotes (<2 µm). In these 2 groups, only cellular chlorophyll *a* (chl *a*) content increased (by 20 and 100%, respectively). The physiological conditions of the 2 to 20 µm cells improved significantly, but a statistically significant (3-fold higher) biomass was observed only in the largest size fraction (8 to 20 µm). Bottle experiment results were comparable with *in situ* results, except that the responses occurred earlier. In addition, the total increase in biomass was much larger than that in the field (100- and 25-fold increase for cell carbon and chl *a* content, respectively). In this respect the control and the iron-enriched bottles showed a comparable trend, suggesting that, next to iron, light was probably a factor of great importance. In the field, phytoplankton cells experience rapidly changing light conditions due to wind-induced turbulence that causes mixing of the water column. In addition to iron-limitation, this results in a generally poor physiological condition of algae in the field. This light-stressor mainly affected the smallest algal size classes (<8 µm). In larger cells, iron enrichment partly compensated for this negative light effect, resulting in a final dominance of larger phytoplankton.

KEY WORDS: Phytoplankton · Iron · Viability · EisenEx

INTRODUCTION

Together with large areas of the equatorial and sub-Arctic Pacific Ocean, the Southern Ocean belongs to the high-nutrient, low-chlorophyll (HNLC) regions (DeBaar et al. 2005), but differs from other low-chlorophyll regions in that its concentration and supply of macronutrients is high enough for phytoplankton blooms comparable to those in coastal regions to occur. In recent years, there has been increasing evidence that not only macronutrients such as nitrate, phosphate and silicate determine the size of the phytoplankton bloom, but also that availability of iron and/or light are crucial. Iron controls the primary productivity in HNLC regions and also acts as a co-limiting factor in all other oceans (Blain et al. 2004). Technological developments have allowed detailed examination of the iron-limitation hypothesis over the past 15 yr (Martin & Fitzwater 1988). The role of iron in cell physiology, and hence in growth and productivity of phytoplankton, has been examined in various experimental set-ups. A direct link between the biological availability of iron and phytoplankton growth has been demonstrated in laboratory experiments with uni-algal cell cultures (e.g. Sunda & Huntsman 1995). In many of these studies, iron speciation was artificially controlled by the addition of chelators such as ethylene-diaminetetraacetate (EDTA). An environmentally more realistic alternative

*Email: veldhuis@nioz.nl

is the incubation of algae with filtered natural seawater free of plankton and particles (Timmermans et al. 2001, 2004). In several cases, the role of iron in phytoplankton bloom formation has been studied during natural iron enrichments experiments in the open ocean (DeBaar et al. 1995, Bucciarelli et al. 2001, Blain et al. 2004). During the past decade, the trend has been to conduct *in situ* experiments using artificial iron enrichment. A good overview of this development is given by DeBaar et al. (2005). Currently, these large-scale *in situ* experiments are considered the best way to test the iron-limitation hypothesis since they allow detailed analysis of the whole suite of chemical and biological parameters. Moreover, they also provide detailed information on the ultimate fate of the newly produced material (Tsuda et al. 2003, Boyd et al. 2004).

With respect to the phytoplankton community, there is consensus that iron addition selectively stimulates the growth of the larger phytoplankton species, particularly diatoms such as *Chaetoceros debilis* (10 to 30 µm), *Pseudo-nitzschia* sp. (a small 2 to 6 µm but long chain-forming species), and the diatom *Fragilariopsis kerguelensis* (10 to 80 µm long). The latter species especially can form large blooms in the Atlantic sector of the Southern Ocean, and experimental evidence has shown a rather low iron affinity, and hence high iron demand, of this large diatom (Timmermans et al. 2001, 2004). However, another prerequisite for the development of blooms of large diatoms is a high concentration of silicate, which is required to construct their frustules. In contrast, the response of the smaller phytoplankton species to iron addition appears to be marginal, suggesting that ambient iron would not limit the growth rates of these smaller algae (Cullen 1995, Boyd et al. 2000, Veldhuis et al. 2005b). In HNLC environments, bloom formation of small phytoplankton would mainly be grazer-controlled. These 2 different controlling factors, dependent on cell size, are known as the 'ecumenical iron hypothesis' (Cullen 1995).

As a consequence of a size-dependent response to the factors controlling biomass, variations in biochemical composition and physiology on the cellular level will also occur. In order to examine these variations in more detail, we studied a variety of cellular parameters in phytoplankton of different size classes (<1 to ca. 20 µm diameter) during the iron enrichment experiment EisenEx conducted in the Atlantic sector of the Southern Ocean. Concomitant with a large-scale *in situ* field trial, laboratory-scale batch-incubation experiments were conducted. Responses were measured as changes in numerical abundance of cells, changes in derived bio-optical properties (measured by flow cytometry) such as cell size and cellular chlorophyll autofluorescence, photochemical efficiency (F_v/F_m) (Schreiber et al. 1993, Gorbunov et al. 1999, Sosik & Olson 2002), and cell viability, measured by examining the integrity of the cellular membrane (Veldhuis et al. 2001). The advantage of using physiological parameters is that, unlike cell numbers, these are relatively independent of grazing pressure and do not require manipulation of the water samples.

MATERIALS AND METHODS

Sampling area. The *in situ* enrichment experiment EisenEx (Eisen-Experiment, ANT-XVIII/2) was carried out from the RV 'Polarstern' in the Southern Polar Frontal zone (~48° S, 21° E). The cruise lasted from 25 October until 5 December 2000. A patch of 50 km^2 within a mesoscale cyclonic eddy, with a diameter of 150 km (Strass et al. 2001), was fertilized with ferrous sulfate solution and marked with an inert tracer (SF6). The fertilized patch was intensively sampled for 21 d. During this period there were 3 iron additions at the center of the gyre (Days 0, 7 and 16), resulting in elevated iron concentrations (from 1 to 2 nmol l^{-1}) (Croot et al. 2005). During the whole sampling period the iron concentration was well above the natural concentration of <0.1 nmol l^{-1}, measured before iron addition. Initial macronutrient concentrations were nitrate > 22 µmol l^{-1}, phosphate > 1.5 µmol l^{-1}, silicate > 12 µmol l^{-1}. Continuous mapping of surface SF6 concentrations ensured correct sampling inside (in-patch) and outside (out-patch) the iron-enriched area (Watson et al. 2001). SF6 measurements provided almost continuous information that was confirmed at a later stage by discrete iron measurements (Croot et al. 2005).

Discrete water samples were taken at different locations inside (in) and outside (out) the iron-enriched area, with a rosette sampler equipped with a CTD unit (Sea-Bird Electronics SBE 911plus) and 24 Niskin bottles. In general, 10 to 12 depths were sampled, covering the upper 200 m of the water column. Sampling outside the iron-enriched area was at different stations outside but near to the fertilized patch. Subsamples were taken in 50 ml bottles for analysis of the phytoplankton composition and cell viability applying flow cytometry (Veldhuis & Kraay 2000) and pulse amplitude-modulated (PAM) fluorometry (Schreiber et al. 1993).

On 2 occasions (7 and 8 November 2000), large-volume (10 l) samples were taken, under ultra-clean conditions, using a towed *in situ* sampler (water taken at 2 m depth, corresponding to 60–70% of surface irradiance). This sampling method has proven to provide uncontaminated surface water samples (DeJong et al. 1998) and was also used during the cruise as the main

sampling source of surface water for the determination of iron (Croot et al. 2005) and SF6 (Watson et al. 2001). The first (control) sample was taken prior to, and the second shortly after, the initial iron enrichment of the surface water. Both samples were incubated in 10 l polycarbonate bottles under ultra-clean conditions inside a special (metal-free) container, mimicking environmental conditions as closely as possible (growth irradiance ~100 µmol quanta m^{-2} s^{-1}, temperature 2°C, 16:8 h light:dark). Phytoplankton composition and physiology were monitored daily. Subsamples were taken for flow cytometric analysis of phytoplankton composition and abundance, viability and PAM fluorometry.

Flow cytometry. Freshly collect CTD bottle samples were routinely analyzed for phytoplankton community composition with a bench-top flow cytometer (Coulter XL-MCL) within 1 h of sampling. Prior to analysis, the samples were stored on melting ice and kept in the dark. Chlorophyll *a* (chl *a*) autofluorescence (emission > 630 nm) and phycoerythrin (PE) autofluorescence (emission = 575 ± 20 nm) were measured in addition to forward scatter (indicator of cell size). The flow cytometer was calibrated using beads of known size (3 and 10 µm) and fluorescence properties on a day to day basis (Veldhuis & Kraay 2000). The flow cytometer remained very stable, despite occasional bad weather, and the signals from the calibration beads varied by no more than 5%.

Unlike specially designed flow cytometers, most commercial instruments are not very suitable for analysis of large and complex cells (Dubelaar & Jonker 2000). Moreover, at a limited sample-flow rate, sample volumes vary from 0.5 to 1 ml. Under these circumstances, an accurate estimation of a low number of large cells would be difficult. In the present study, a cell size of ca. 20 µm was the operational upper size-limit of the phytoplankton community that could be quantified in reliable numbers.

Flow cytometric analysis of the phytoplankton community showed, in general, 5 major groups. Based on PE fluorescence and cell size (equivalent spherical cell diameter [ESD] of 1 to 1.5 µm), this group was classified as *Synechococcus* spp. Other phytoplankton species which could be identified to the species level and confirmed microscopically were a chain-forming *Pseudo-nitzchia* species (ca. 4 µm wide but >100 µm in length), and colonies and single cells of *Phaeocystis antarctica*. The high number of cells, occasionally observed, was probably due to disruption of *P. antarctica* colonies when passing through the nozzle of the flow cytometer (Veldhuis et al. 2005a).

Phytoplankton cell size, carbon and chl *a* biomass. Cell size of the different phytoplankton clusters identified by flow cytometry was determined in a series of fractionated samples (10, 8, 5, 3, 2, 1, 0.6, and 0.4 µm, cf. Veldhuis & Kraay 2000). For each cluster (in the case of *Synechococcus* spp. for a species), the number of cells retained after each filtration step was measured and plotted as a function of filter pore-size. In a fitted S-shaped plot, the ESD was determined as the size displayed by the median (50%) of the cell number retained. This procedure was repeated several times during the enrichment experiment. Based on these flow cytometer data and fractionation experiments, 4 clearly defined clusters of eukaryotic phytoplankton were assigned in addition to *Synechococcus* spp.: (1) pico-eukaryotes with an ESD of <1.5 µm (hereafter referred to as pico-Euk); (2) small eukaryotes with an ESD ranging from 1.5 to 3.5 µm (EukI); (3) eukaryotes with an ESD ranging from 3.5 to 8 µm (EukII); and (4) a group of large eukaryotes (EukIII) consisting of a mixture of cells varying considerably in size (ESDs ranging from 8 to 20 µm) and in chl *a* autofluorescence.

The size parameter derived by flow cytometry (forward light scatter) showed a linear relationship with the ESD determined by the fractionated filtration procedure (Fig. 1A). This linear relationship was used to estimate the ESD of the different algal groups in each sample. Cell biovolume was then calculated assuming a spherical cell (cf. Gall et al. 2001) and phytoplankton cell carbon using the carbon to volume relationships of Verity et al. (1992). In the present study, phytoplankton cell volumes varied over 3 orders of magnitude. Therefore, 3 different carbon densities were used: 0.36 pg C $µm^{-3}$ for a cell volume < 10 $µm^3$, 0.24 pg C $µm^{-3}$ for a cell volume ranging from 10 to 100 $µm^3$, and 0.16 pg C $µm^{-3}$ for a cell volume of 100 to 1000 $µm^3$ (Verity et al. 1992).

In a similar way, a factor was established for converting the flow cytometrically derived chl *a* autofluorescence into cellular chl *a* content (Fig. 1B). Chl *a* values were chemically determined for the whole phytoplankton community and, on numerous occasions, for the <20 µm fraction both inside and outside the iron-enriched area (Gervais et al. 2002). These chl *a* values showed a statistically significant linear relationship with the chl *a* autofluorescence determined by flow cytometry, with the exception of the total phytoplankton community inside the iron patch (Fig. 1B). Towards the end of the *in situ* experiment, the chemically determined chl *a* content exceeded flow cytometry values by a factor of 2 to 3. This was entirely due to a proportional increase in phytoplankton >20 µm (Gervais et al. 2002), which were not measured by flow cytometry. Based on the present results, we conclude that the flow cytometer in its current design does quantify the phytoplankton community in the size range 0.6 to 20 µm. Applying the conversion factor for chl *a* autofluorescence to chl *a*

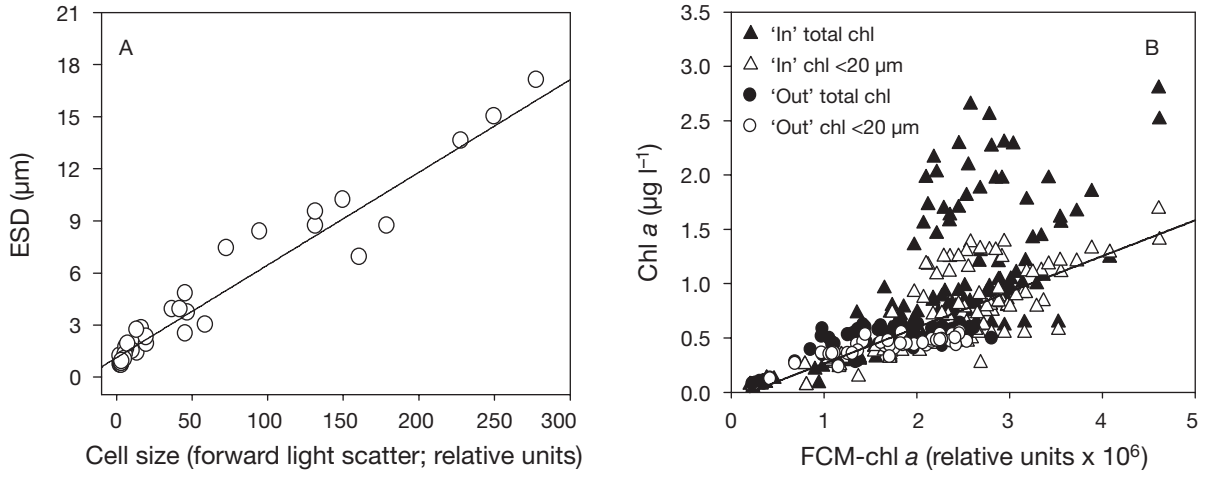

Fig. 1. (A) Variation in equivalent spherical diameter (ESD) as a function of cell size determined by flow cytometry (forward light scatter, FLS). ESD = 0.0534 × FLS + 1.1245 (r^2 = 0.9366, n = 42, $p < 0.001$). (B) Variation in chl *a* concentration of total phytoplankton community and of <20 µm size fraction inside (in) and outside (out) iron-enriched area vs. chl *a* autofluorescence biomass determined by flow cytometry (FCM). Chl *a* (<20 µm) = 3.223×10^{-6} FCM-chl *a* – 0.0752; (r^2 = 0.7909, n = 167, $p < 0.01$), whereby <20 µm fraction includes data from inside and outside the iron-enriched area

content, and assuming that group-specific chl *a* autofluorescence represents a proportional fraction of the total chl *a* content, chl *a* values for the different phytoplankton size categories were determined for each sample. Combined with the carbon values it was possible to calculate Φ, the cell carbon:chl *a* ratio, providing information on the chl *a* density of the different phytoplankton size classes.

Phytoplankton viability. The relative percentage of live cells in the different phytoplankton clusters was measured by testing the integrity of the cell membrane (Veldhuis et al. 2001, Casotti et al. 2005). This integrity test is based on the inability of the nucleic acid specific stain SYTOX Green (S-7020; Molecular Probes) to pass into cells with intact plasma membranes. We added 10 µl ml^{-1} of working solution to 1 ml of sample, yielding a final dye concentration of 0.5 µM. Samples were incubated for 15 min on ice in the dark prior to flow cytometric analysis of the DNA/green fluorescence of each phytoplankton cluster. Cells were considered non-viable when their DNA/green fluorescence signal (emission = 525 ± 20 nm) exceeded any background-green autofluorescence (determined in the unstained sample) by at least 5-fold (cf. Veldhuis et al. 2001). The viability of phytoplankton >8 µm (EukIII) was not determined in this assay, since their cell numbers were too low for reproducible and statistically significant data.

Photochemical quantum efficiency. The photochemical efficiency of photosystem II (F_v:F_m) of the whole phytoplankton community was measured using the pulse amplitude-modulated fluorometer (Water-PAM, Walz). Freshly collected samples were stored on ice in the dark for at least 30 min prior to measurement. Minimum (F_0) and maximum (F_m) fluorescence levels, were measured to calculate F_v (variable fluorescence, $F_v = F_m - F_0$) and F_v:F_m (Schreiber et al. 1993).

The same procedure was used for different fractions collected in the size-fractionation experiments (cf. Cermeño et al. 2005). Numerical abundance and group-specific chlorophyll biomass were determined by flow cytometry for each subsample. Subsamples were measured at least 3 times and for the F_v:F_m measurements using at least 5 replicates and 5 blanks (cf. Cullen & Davis 2003). Using both data sets, it was possible to calculate the F_v:F_m for each algal population.

This method is based on the assumption that the relative contribution of each phytoplankton group to the average F_v:F_m of the whole community is proportional to its chlorophyll biomass and its specific F_v:F_m. Furthermore, gentle filtration does not alter the physiological properties of the different groups. For any number of phytoplankton groups present Eq. (1) can be used to determine total and group-specific F_v:F_m:

$$\frac{\sum_{i=1}^{n} P_i (F_v : F_m)_i}{\sum_{i=1}^{n} P_i} = \overline{F_v : F_m} \quad (1)$$

where P_i = group-specific chlorophyll biomass (cell number multiplied by cellular chl *a* autofluorescence), $(F_v:F_m)_i$ = group-specific photosynthetic activity, $\sum_{i=1}^{n} P_i$ = total phytoplankton biomass of different groups (n), and $\overline{F_v : F_m}$ = weighted average photosynthetic activity (in practice the community average value normally measured with the PAM fluorometer on an intact undisturbed sample).

Each filtration step removes certain size classes of cells, and thus also its contribution to the average photochemical efficiency of the phytoplankton community.

The exact numbers and chlorophyll biomass of the remaining size groups is determined by flow cytometry. This stepwise subtraction method generates a set of equations with a declining number of phytoplankton groups, with consequent changes in average F_v:F_m of the community. This results in a matrix of varying number of size groups and average community values for F_v:F_m. The group-specific F_v:F_m is computed by multiple regression analysis with optimal fit, a standard regression tool within Excel (Microsoft). The community average calculated using the computed group-specific values yielded a value for F_v/F_m that differed by maximally 15% from the actual measured value of the unfiltered sample.

This fractionation and regression analysis approach is an indirect method of calculating size-specific photochemical efficiency and differs from other methods whereby the quantum yield of photochemistry of each individual cell is measured (Gorbunov et al. 1999, Olson et al. 2000).

RESULTS

The mesoscale eddy was 100 to 150 km in diameter and enriched with iron 3 times during our study: on Days 0, 7 and 16. The added iron was dispersed downwards and laterally by strong winds and 2 major storms. As a result, the wind-mixed upper layer was on average 40 to 50 m thick and increased during storms to >100 m (Gervais et al. 2002, DeBaar et al. 2005). The initial iron-enriched patch in the cyclonic eddy of 50 km^2 had increased to ca. 950 km^2 at the end of the survey at Day 21.

During this study the dynamic size range of the phytoplankton community exceeded 3 orders of magnitude (from <1 to >1000 µm). The smallest picophytoplankton species possessed an ESD of only 0.7 µm. Based on its pigment signature, the species was probably a prymnesiophyte (I. Peeken pers. comm.). The cell size of the species was only slightly larger than that of *Prochlorococcus* spp. Moreover, the DNA content of intact cells was also 1.7 times that of *Prochlorococcus* spp., indicating that the observed picophytoplankton species belongs to the smallest known pico-eukaryotes.

Large diatom species such as *Fragilariopsis kerguelensis*, *Corethron* spp, *Pseudo-nitzchia* sp. and colonies of *Phaeocystis antarctica* were observed towards the end of the experiments (U. Freyer & P. Assmy pers. comm.). The size class >20 µm (Fig. 1B) increased in importance from Day 8 onwards, resulting in a contribution of up to 40% of the bulk chl *a* at the end of the survey at Day 21 (Gervais et al. 2002).

Fig. 2A (in patch area) shows the vertical distribution of the phytoplankton as total numerical cell abundance, *Synechococcus* spp., and 4 other size-classes, corresponding to clearly identifiable clusters of phytoplankton during the different stages of the *in situ* experiment. The profiles presented are 5 out of a series of 15 covering the whole 21 d period, highlighting the major features observed. The total number of the phytoplankton cells as well as that of the different size groups during the whole field campaign inside the iron-enriched patch did not deviate significantly from the range found outside the iron-enriched patch (Fig. 2). Furthermore, in both regions a significant fraction of the phytoplankton community was found below the euphotic zone (z_{eu}), varying outside and inside the iron-enriched patch from 20% during the first week to 70% at the end of the survey.

The vertical profiles also showed 2 general trends highly correlated with prevailing weather conditions. During periods of strong winds, the upper water layer was thoroughly mixed, resulting in constant cell numbers for all size groups in the upper 40 to 60 m (e.g. Days T–1 and T15.3). During periods of calm weather, the highest abundance of the small phytoplankton (pico-Euk and EukI), showed a surface peak gradually declining with depth (Days T3.8 and T10.5), indicative of active growth in the surface layer. In contrast, the larger cells (>8 µm, EukIII), occasionally showed subsurface maximum abundance. Remarkably, cell numbers of *Synechococcus* spp. (belonging to the picophytoplankton group) were almost unaffected by changes in the physical structure of the water column, and their numerical abundance remained virtually constant in the upper 100 m.

The first clear indication of stimulation of chl *a* synthesis by iron enrichment was an increase in cellular chl *a* autofluorescence, observed at Day T10.5 (Fig. 3A). For most phytoplankton size classes, the chl *a* autofluorescence signal continued to increase until the end of the survey on Day 21 (T21.2). The magnitude of the increase in cellular chl *a* content, however, was cell size-dependent and was mainly restricted to the surface layer inside the iron-enriched area (Fig. 3, Table 1). An exception was the larger phytoplankton fraction (EukIII), for which the chl *a* autofluorescence per cell had increased also in the deeper layers (>60 m) by the end of the experiment (T21.2). For *Synechococcus* spp., this increase was only 20% over the initial values and those outside the iron patch. For the 2 smallest groups of eukaryotes (pico-Euk and EukI), chl *a* autofluorescence increased by a maximum factor of 2, for the larger algae (EukII) by 2.5 to 3.5, and for the largest group (EukIII) by 3.5 to 4. On average, the cellular chl *a* autofluorescence of the whole phytoplankton community increased by a factor of 2. For the smaller-sized component of the phytoplankton community (cell diameter < 3 µm), chl *a* autofluorescence

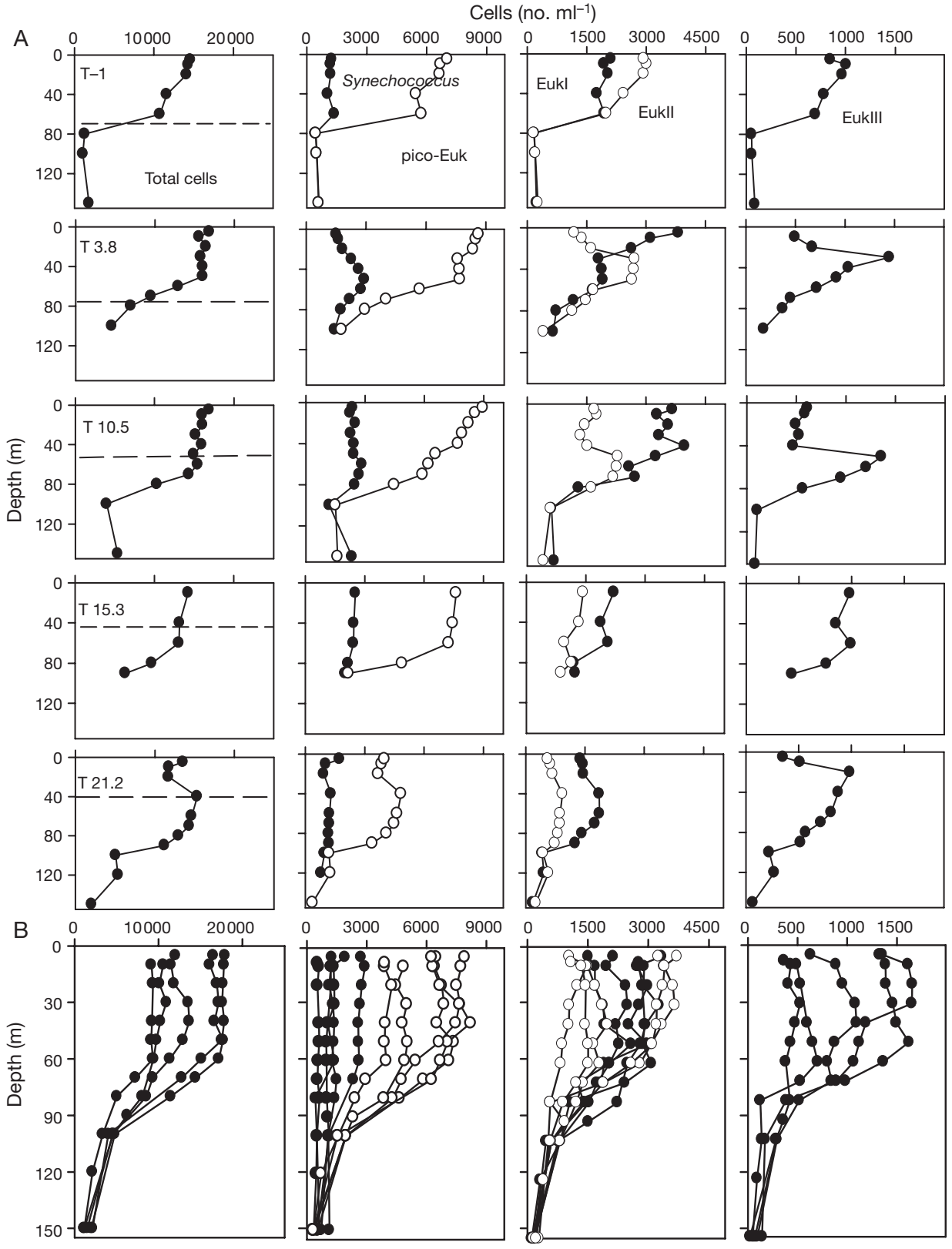

Fig. 2. Numerical abundance of *Synechococcus* spp., pico-Euk, EukI, EukII, and EukIII at (A) a few stations (5 from a total of 15 profiles) inside and (B) 5 stations outside the iron-enriched area as a function of depth. Sampling days (T) are indicated as time after the first iron enrichment; T–1 is day before first enrichment. Dashed lines indicate depth of euphotic zone (1% of surface irradiance depth: I_d 1%)

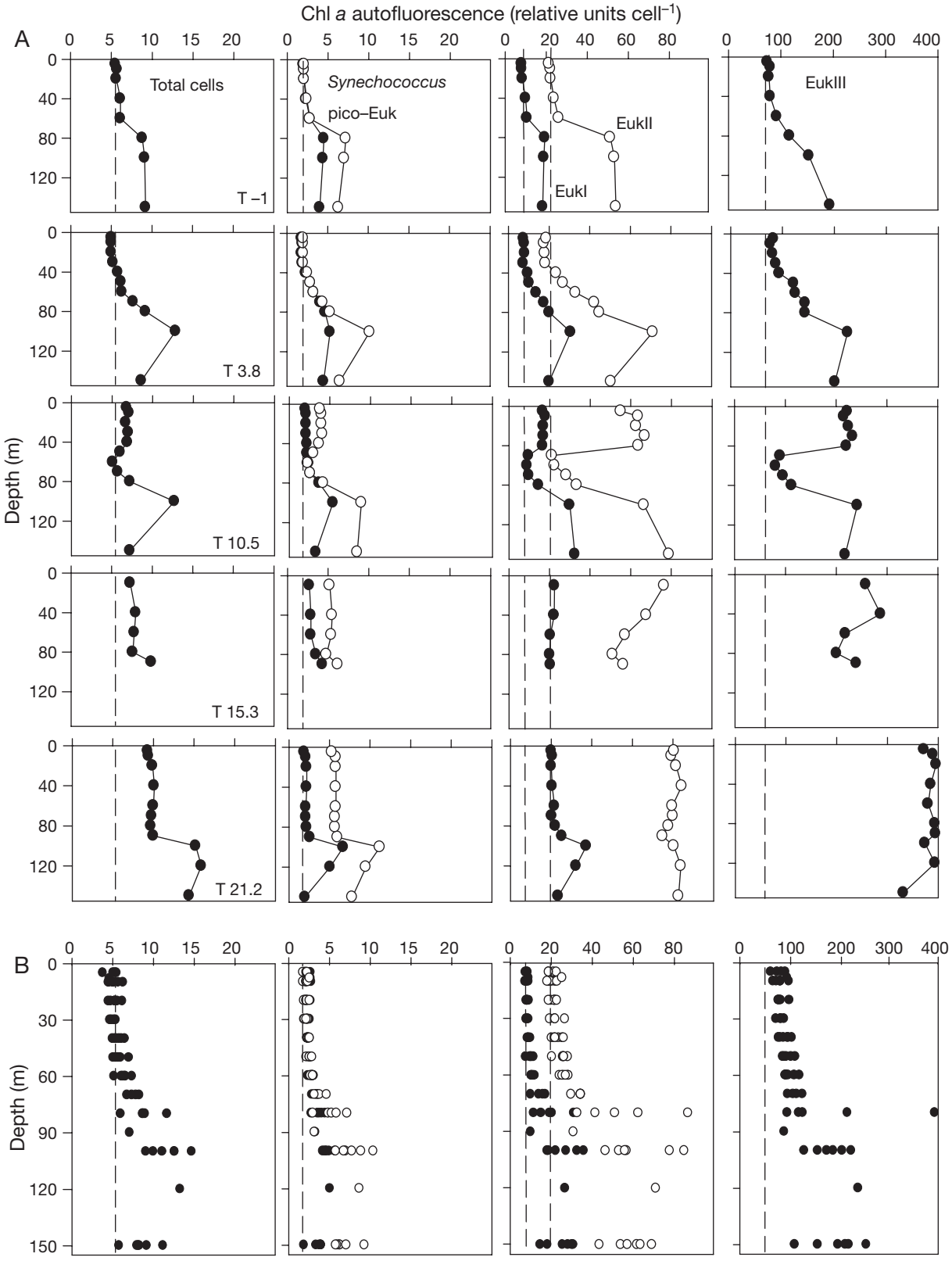

Fig. 3. Vertical distribution of cellular chl *a* autofluorescence of different size classes of phytoplankton on 5 different days of bloom development (A) inside and (B) outside the iron-enriched area. Dashed lines indicate values measured at the surface on Day T–1 for each phytoplankton group. For details of sampling days and clarification of symbols see Fig. 2

Table 1. Mean (±SE) population-specific photosynthetic efficiency (F_v:F_m). F_v:F_m of unfiltered phytoplankton community was 0.32, 0.50 and 0.57 on Days T–1, T9 and T20, respectively. Chl *a*: chl *a* content (based on Fig. 1B); Live cells: minimum and maximum values of 4 to 5 samples taken in upper 30 m of water column at the stations. Samples taken at 20 m (T–1 and T20) and 40 m (T9); nd: not determined

	F_v:F_m	Chl *a* (fg cell^{-1})	Live cells (%)
T–1			
Synechococcus spp.	0.31 (0.16)	6.5	42–57
Pico-eukaryotes (<1.5 µm)	0.09 (0.08)	5.6	57–61
Eukaryotes			
EukI (1.5 to 3.5 µm)	0.10 (0.06)	39.6	30–41
EukII (3.5 to 8 µm)	0.54 (0.18)	131	40–55
EukIII (>8 µm)	0.37 (0.24)	556	nd
T9			
Synechococcus spp.	0.03 (0.17)	8.7	55–61
Pico-eukaryotes (<1.5 µm)	0.09 (0.14)	8.5	50–54
Eukaryotes			
EukI (1.5 to 3.5 µm)	0.32 (0.61)	75.9	52–61
EukII (3.5 to 8 µm)	0.61 (0.29)	286	79–85
EukIII (>8 µm)	0.60 (0.18)	1541	nd
T20			
Synechococcus spp.	0.03 (0.18)	9.4	50–62
Pico-eukaryotes (<1.5 µm)	0.12 (0.06)	8.3	58–70
Eukaryotes			
EukI (1.5 to 3.5 µm)	0.45 (0.14)	65.8	52–62
EukII (3.5 to 8 µm)	0.59 (0.10)	317	75–84
EukIII (>8 µm)	0.60 (0.08)	1257	nd

increased in the euphotic zone only, and always remained well below the values in deeper water layers. In contrast, iron addition increased the cellular chl *a* content of the larger phytoplankton cells at the sea surface to values exceeding those in deeper water samples (Fig. 3A). Occasionally and mainly in the first 2 wk (e.g. Fig. 3A, T10.5), a subsurface minimum occurred, indicating that enhanced chlorophyll synthesis was restricted to the higher light levels. This feature arose mainly from a water mass with a surface layer enriched in iron overlying a deeper (unenriched) water layer (Croot et al. 2005).

Based on the flow cytometry data on cell size, cell biovolume was determined and combined with volumetric-dependent carbon densities (Verity et al. 1992). Group-specific carbon content was calculated from these data (Fig. 4A,B). The trends in carbon content during the course of the *in situ* experiment showed a strong resemblance to those for cell abundance (Fig. 2). The total carbon concentration of EukI showed a temporal increase in the first 13 d at the surface, resulting more from an increase in cell numbers than from an increase in cell carbon. After this period, the carbon concentration of this group declined again to the original values, similar to those outside the iron-enriched area. Carbon content of the large phytoplankton (mainly EukIII > 8 µm) increased moderately in the second half of the experiment; this increase started at the surface but, from T15.3 onwards, was also observed for deeper water layers.

Φ (Fig. 4A,C) for 3 of the size classes (*Synechococcus* spp., EukI and EukII) showed only minor variation over time, both outside and inside the iron-enriched patch. Only 2 groups (pico-Euk and EukIII) showed a gradual decline in Φ throughout the survey, but this was restricted to the surface layer. This response was primarily caused by an increase in the cellular chl *a* content relative to cellular carbon content.

For all algal groups, highest Φ values were at the surface; in the euphotic zone these declined slightly with increasing depth, whereas below the euphotic zone the decline was much sharper, primarily because of enhanced cellular chl *a* synthesis of the algal cells (see also Fig. 3). Throughout the water column Φ varied by a factor of 2 to 3 for all groups, with declining values from the surface to deeper waters. An exception was the largest size class (EukIII) towards the end of the survey. In surface waters, the Φ of EukIII declined steadily over time, resulting in a surface minimum at the end of the survey.

Area estimates of total carbon, chl *a*, and Φ showed little variation over time for all size classes (Fig. 5A–C), with the exception of the largest phytoplankton group examined (EukIII). In terms of carbon and chl *a* biomass, the larger algae were and remained the dominant group. The second dominant group was the algal size class of 3 to 8 µm (EukII). The 3 phytoplankton groups with the lowest biomass were those with the smallest cell sizes. With little or no change in both chl *a* and carbon biomass, Φ of the 3 smallest phytoplankton groups also varied little, ranging between 12.5 ± 1.4 and 15.4 ± 2.4 mg C (mg chl *a*)$^{-1}$ (mean ± SE). Values of Φ for *Synechococcus* spp. were slightly higher at 21.6 ± 3.4 mg C (mg chl *a*)$^{-1}$. Finally, the highest values were found for the larger eukaryotes (EukIII), with a mean value of 36.3 ± 7.5 mg C (mg chl *a*)$^{-1}$. This implies that the chl *a* density (chl *a* per unit of carbon) in larger cells is, on average, less than in smaller phytoplankton cells.

The percentage of live phytoplankton cells (i.e. cells with an intact cell membrane) showed some distinct differences between the picophytoplankton (*Synechococcus* spp. and pico-Euk) and the larger algae (EukI and EukII) (Fig. 6). The percentage of viable cells in the picophytoplankton size class remained fairly constant over the whole sampling period, with a percentage of live cells varying between 49 and 70% of the total population size. The initial percentage of live

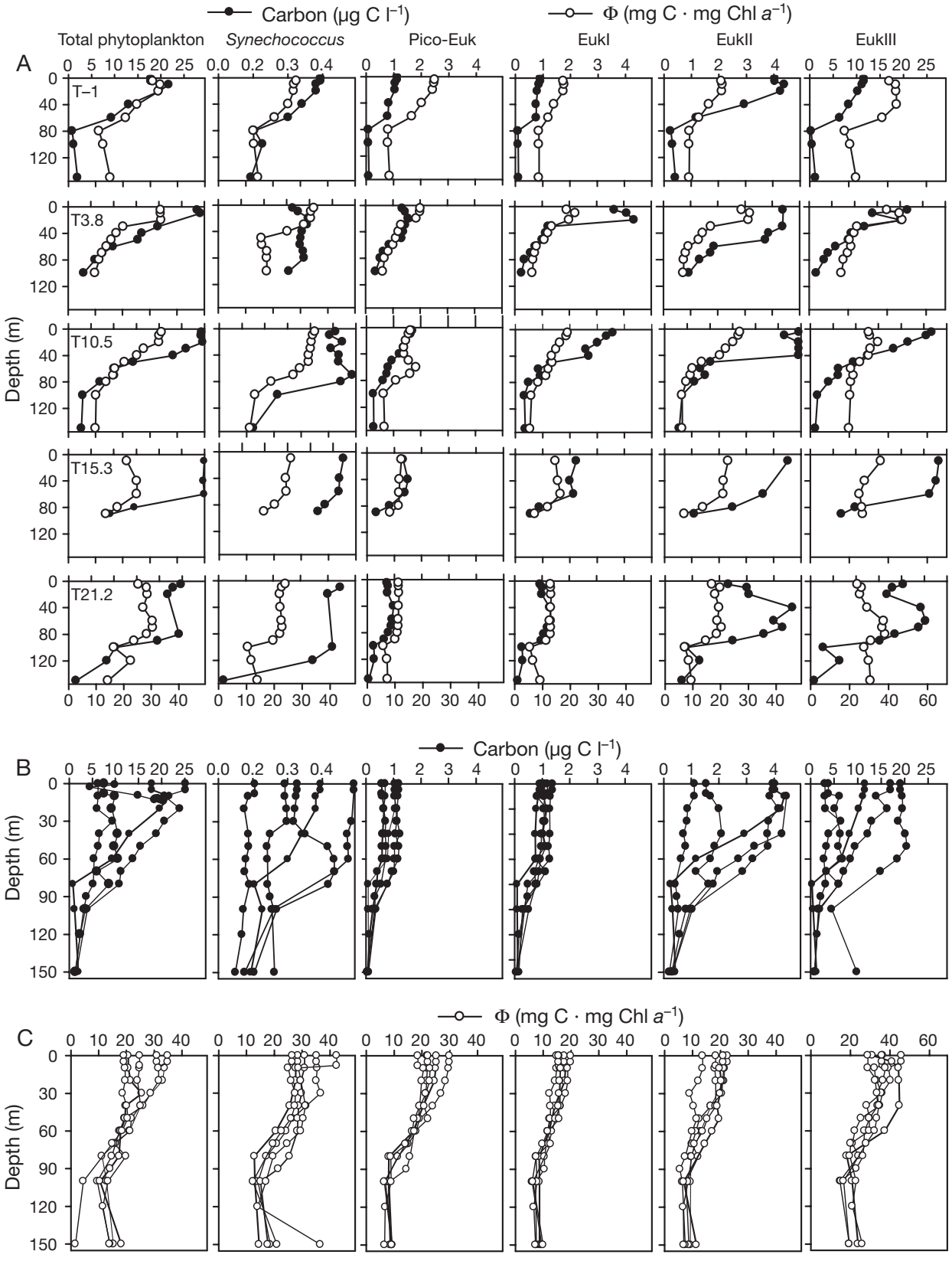

Fig. 4. Vertical distribution of carbon and carbon to chl *a* ratio (Φ) of total and size-class-specific phytoplankton on 5 different days of the bloom development (A) inside and (B,C) outside the iron-enriched area. For details of sampling days see Fig. 2

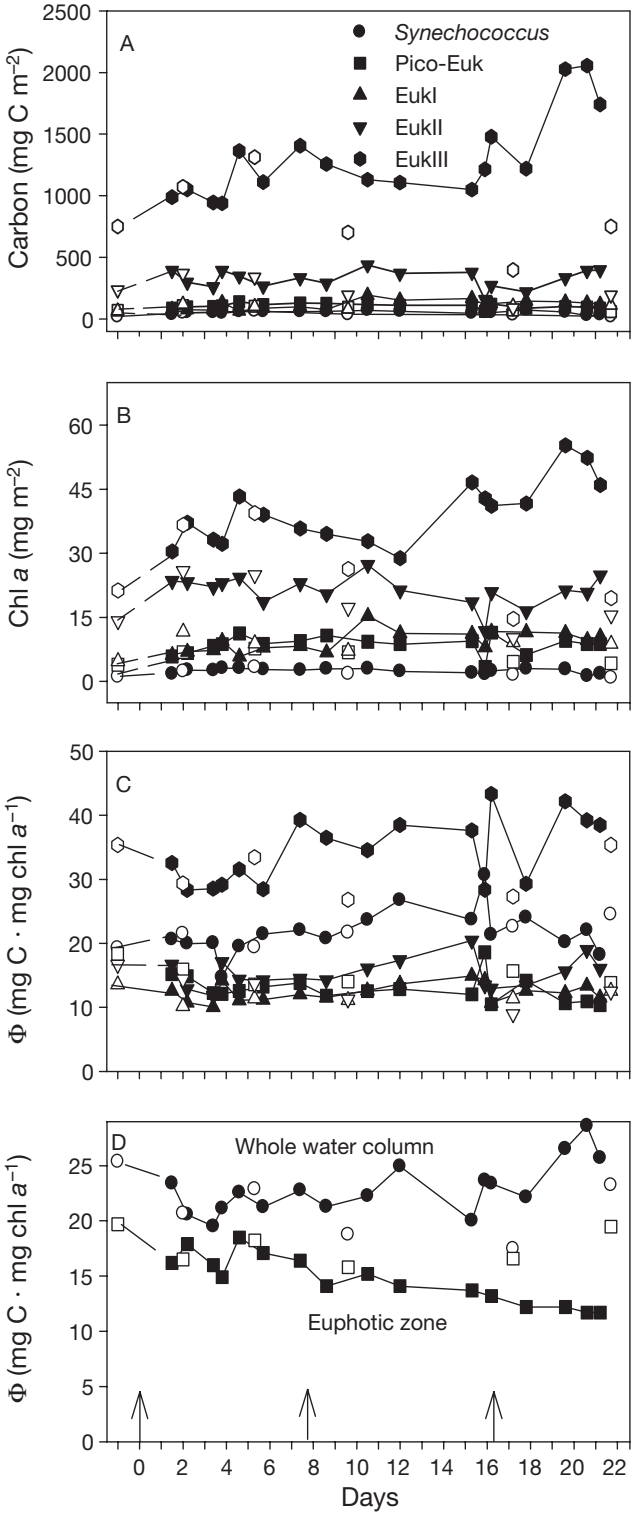

Fig. 5. Area values of (A) phytoplankton size-class-specific carbon, (B) chl *a*, (C) Φ, and (D) whole water column versus euphotic zone values of Φ. Sample days cover the whole sampling period. Closed symbols indicate stations sampled inside the iron-enriched area and open symbols those sampled outside. Arrows at the bottom of (D) mark the times of 3 iron infusions

cells of EukI was only 35% and that for EukII 45% at the start of the experiment, much lower than that of the picophytoplankton. At the end of the survey, this percentage had increased significantly to ca. 60% (EukI) and 80% (EukII).

The percentage of live cells did not show a consistent pattern for the various phytoplankton groups with depth or over time. After several sampling days, a distinct surface minimum was observed, but on other occasions there was a gradual decline in the percentage of viable cells with depth.

Size-class-specific photosynthetic efficiency

On 3 different days (T–1, T9 and T20), a detailed size-fractionated analysis of the F_v:F_m was made of samples taken from the surface mixed water layer (20 or 40 m). In combination with the flow cytometric determined size-class distribution and biomass, a group-specific F_v:F_m was calculated for each of the different phytoplankton groups (Table 1). The F_v:F_m of the whole phytoplankton community increased from a moderate value of 0.32 prior to iron enrichment to a high value of 0.50 at Day 9 and remained high until Day 20 (0.57). The F_v:F_m of the various phytoplankton groups showed remarkable variation between the different size classes and over time. The F_v:F_m of the 3 smallest phytoplankton groups (*Synechococcus* spp., pico-Euk and EukI) were low to very low prior to iron infusion. Of these 3 groups, only EukI showed a major increase (factor 4.5) after iron enrichment. In the other 2 groups, F_v:F_m remained nearly constant (pico-Euk) or declined (*Synechococcus* spp.). Of the 2 larger algal groups, the EukII maintained a high F_v:F_m throughout the whole survey, whereas it increased from low to high within 9 d and remained high until the end of the survey (Day 20) for the largest size class examined (EukIII). In this respect our size-class response differed from previous studies in the equatorial Pacific Ocean (Kolber et al. 1994) and during SOIREE in the Southern Ocean (Boyd & Abraham 2001), where all algal size classes responded similarly.

All size classes showed an increase in chl *a* content per cell (Table 1). The magnitude of these increases covaried to some extent with the observed trends in F_v:F_m, showing the highest increases in the largest size classes. Only *Synechococcus* spp. showed an opposite trend of a reduction in F_v:F_m while the chl *a* per cell increased slightly over time.

Similarly, the viability of phytoplankton cells matched the trend observed for F_v:F_m. In the 2 smallest size classes of phytoplankton groups the percentage of live cells remained nearly constant over time (*Synechococcus* spp. and pico-Euk; see also Fig. 6). In con-

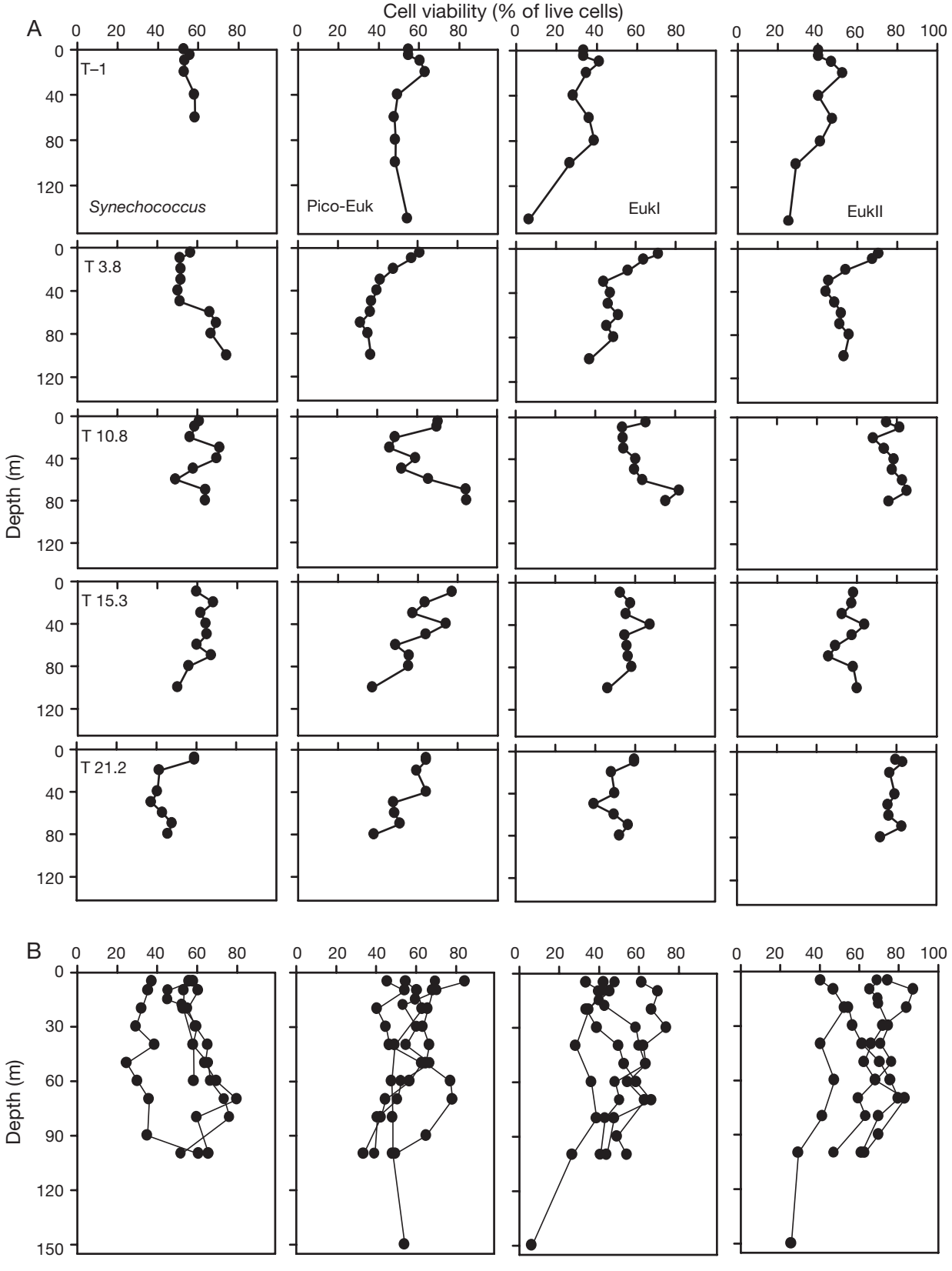

Fig. 6. Vertical distribution of cell viability of 4 different size classes of phytoplankton on 5 different days of bloom development (A) inside and (B) 4 stations outside the iron-enriched area

trast, the percentage of live cells of the phytoplankton groups EukI and EukII increased, and this increase was accompanied by increases in F_v:F_m and chl *a* content per cell.

Incubation experiments

In contrast to the field experiment, with its patchy distribution of the phytoplankton community, the phytoplankton in the 10 l bottles showed a clearer development of the different groups and their physiological properties. (Fig. 7B). Total phytoplankton cell numbers increased gradually by a factor of 2 in the control bottle and 3-fold in the iron-enriched one over the first 6 d. In the subsequent 15 d, total phytoplankton cell abundance declined gradually to a value identical to that at the start of the experiment. Concentrations of nutrients (silicate, nitrate and phosphate) declined gradually (Fig. 7A). From Day 15 onwards nutrients were nearly depleted, starting with silicate, in the iron-enriched bottle, while the control bottle contained residual nutrients throughout the incubation (up to Day 21).

Measurements of the phytoplankton F_v:F_m of the whole community showed a sharp drop of 30% the first day after transfer of the field samples into the bottle, and it took another 2 d for a full recovery to the original value (Fig. 7F). From Day 3 onwards, the F_v:F_m increased further in both bottles but in a different manner. In the control bottle, the F_v:F_m increased only 70%, but in the iron-enriched bottle the F_v:F_m increased by as much as 130% compared to the initial values. These elevated F_v:F_m ratios were maintained for another 7 d. Subsequently, F_v:F_m declined to the initial value in the iron-enriched bottle, but to a value only 2-fold lower than the initial value in the control bottle. This decline coincided with the sharp reduction in the concentration of the various macronutrients (Fig. 7A).

Phytoplankton biomass, carbon, and chl *a*, increased rapidly, but occurred after the numerical peak of the phytoplankton (Fig. 7C,D). Carbon values in both bottles increased from ca. 20 to a maximum of 2000 µg C l^{-1}. The chl *a* biomass increased by a factor 25 in the iron-enriched bottle, but only 14-fold in the control. Φ varied, largely due to changes in chl *a*, both between treatments and also over time. In the iron-enriched bottle, the maximum increase of Φ was a factor 4, while in the control it was a factor 11 (Fig. 7E).

The population dynamics showed considerable differences between the various size classes during the course of the experiment (Fig. 8). Of the 5 groups of phytoplankton identified, 3 (*Synechococcus* spp., EukI, and EukII) showed minor changes in numerical abun-

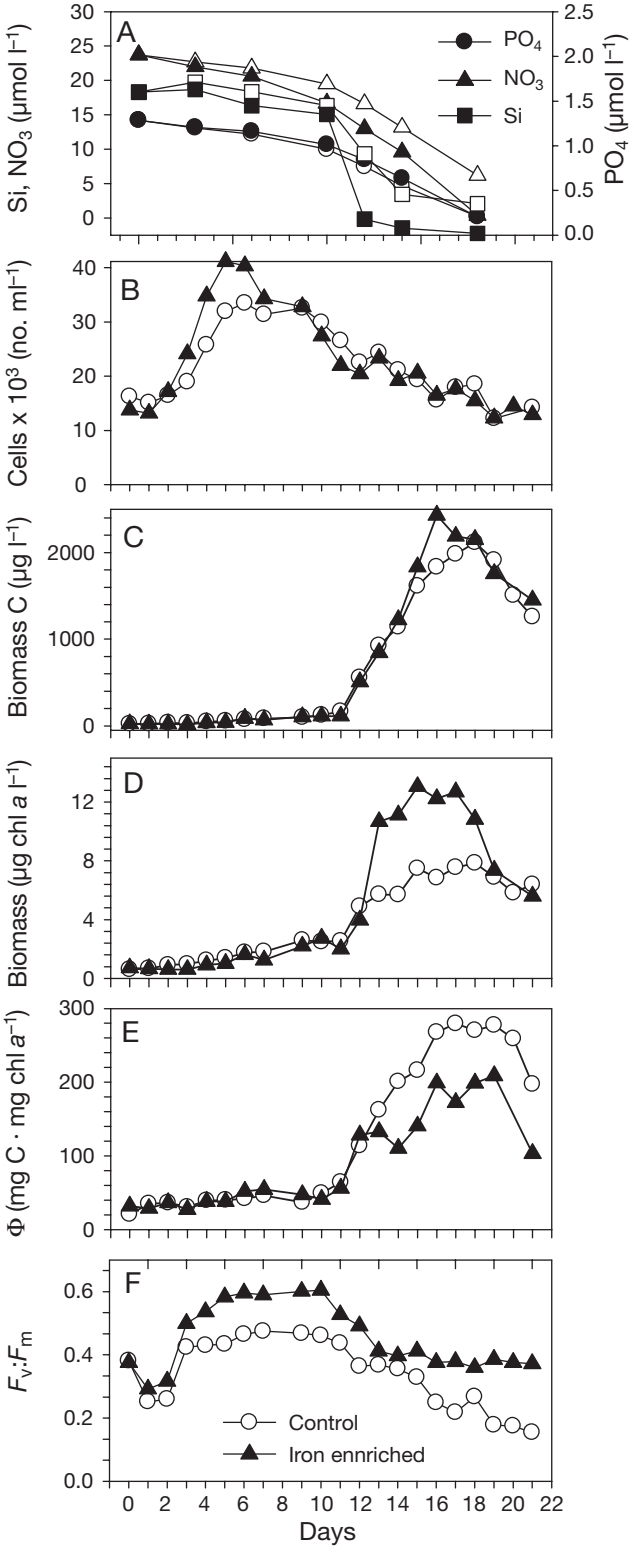

Fig. 7. (A) Nutrient concentrations, (B) total cell numbers, (C) total phytoplankton carbon, (D) chl *a* biomass, (E) Φ, and (F) photosynthetic efficiency (F_v:F_m) in iron-enriched water (closed symbols) and control bottle (open symbols). Day 0 is time of sampling for both bottles, since both bottles were filled at the same location but with 1 day difference

dance. In contrast, the group of pico-Euk showed a 3.5-fold increase in the first 6 d, followed by a similar decline thereafter, resulting in a constant but relatively low value of ca. 1000 cells ml^{-1}. The cell numbers of EukIII increased steadily in the control bottle by a factor of 2, comparable to the dynamic range observed in the field, whereas in the iron-enriched bottle, numbers increased 6-fold starting after a lag-phase of 10 d. As a result, EukIII increased in importance over time in terms of carbon. At the start of the incubation, the relative contribution of this size class was 50%, but had increased to nearly 90% of the total phytoplankton carbon by the end of the experiment (data not shown).

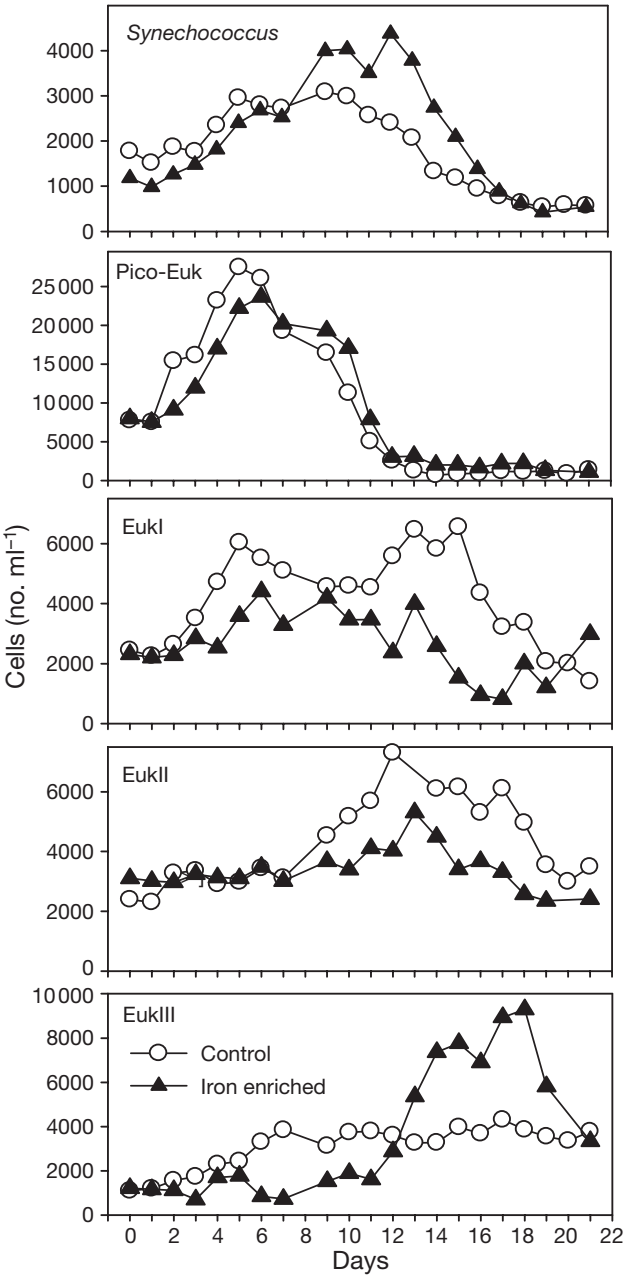

Fig. 8. Numerical abundance of 5 different size classes of phytoplankton in iron-enriched water (closed symbols) and control bottle (open symbols)

The cellular chl *a* autofluorescence of all algal groups remained fairly constant the first 5 d (Fig. 9). In the following period, the fluorescence signal of the smallest algal groups still remained unchanged (*Synechococcus* spp.) or dropped slightly (pico-Euk), independently of iron addition. In the larger algal groups, EukII and EukIII, the cellular chl *a* autofluorescence increased gradually by a factor 2 and 6, respectively. These increases were observed in both bottles and therefore independent of the iron concentration.

The Φ of the 3 smallest size classes remained constant, or in the case of EukI reduced by a factor of 2 during the incubation (Fig. 9B). A clear response of iron enrichment was only observed for pico-Euk, showing a temporary increase in Φ by a factor of 2. In the EukII size class (3.5 to 8 µm), Φ remained constant in the control bottle, with the exception of a temporary drop around Day 10. In the iron-enriched bottle, Φ increased gradually, resulting in a ca. 30% increase compared to the control. Finally, the greatest changes were observed in the largest algal size class (EukIII). From Day 10 onwards, Φ of this algal group increased by a factor of 5 in the iron-enriched bottle and a by factor of 8 in the control.

The percentage of live cells in 3 out of 4 groups increased rapidly within the first 2 d of the incubation (Fig. 10). In the following 12 d, with exception of the pico-Euk in the control bottle, this percentage remained high (70 to 80%). Thereafter, clear differences were observed between the various phytoplankton groups as well as between the control and the iron-enriched bottles. In the case of *Synechococcus* spp., reduction in percentage of live cells coincided with a reduction in cell numbers (Fig. 8). In pico-Euk the percentage of live cells continued to increase in both bottles despite the fact that cell numbers dropped sharply and this size class nearly became extinct towards the end of the incubation (Fig. 8). In EukI and EukII, the percentage of live cells declined during the second half of the experiment. In the iron-enriched bottle this percentage dropped to below the initial value, accompanied by an actual decline in total cell numbers (Fig. 8).

DISCUSSION

The data presented corroborate the results of a variety of studies that test the iron-limitation hypothesis in the Southern Ocean *in situ* (Cavender-Bares et al. 2001), during shipboard incubations (Buma et al. 1991, DeBaar & Boyd 2000, DeBaar et al. 2005) and using

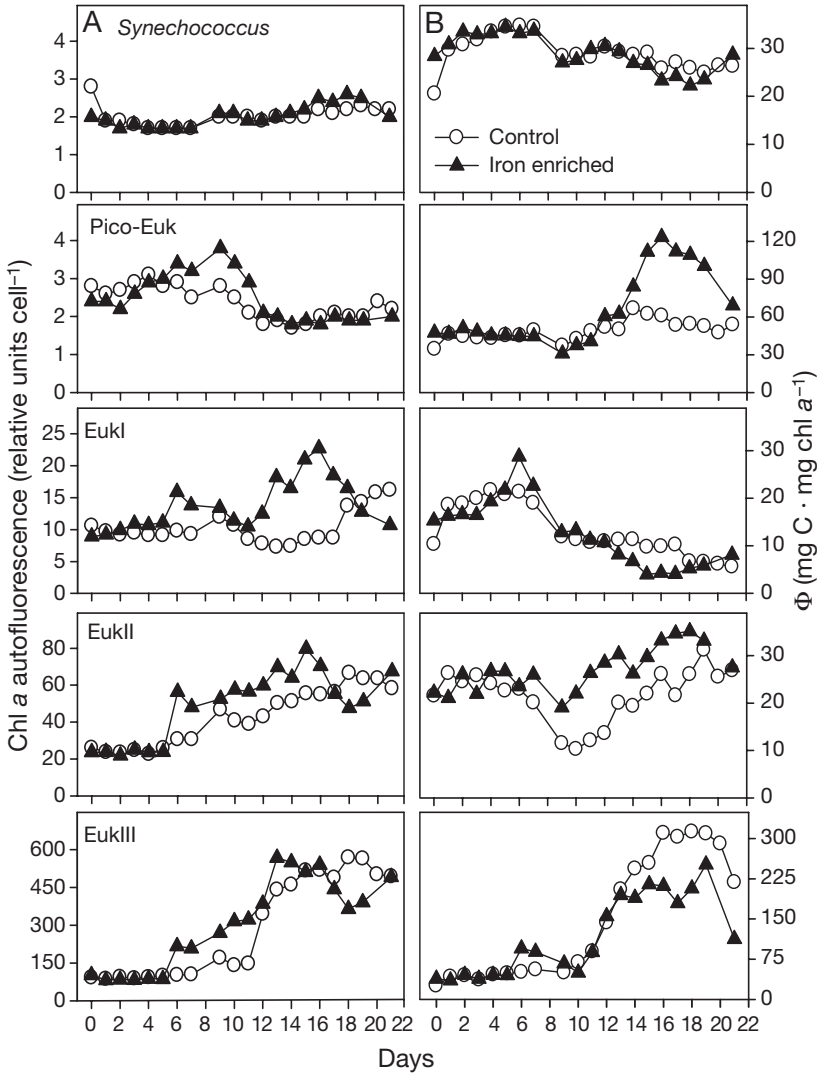

Fig. 9. (A) Cellular chl *a* autofluorescence, and (B) Φ of 5 different size classes of phytoplankton in iron-enriched and control bottle

unialgal cultures (Timmermans et al. 2001, 2004). In our study, iron stimulated phytoplankton <20 µm in size, but mainly the larger sized phytoplankton, in particular diatoms. Colonies of *Phaeocystis antarctica* were also present, but only in low numbers. The effect on abundance of the smaller phytoplankton (<8 µm) was less pronounced (by a factor of <3) than that on the abundance of the larger size-fraction. Size-related growth responses to iron enrichment varied as a function of the biochemical and physiological properties of the phytoplankton (indicative of physiological cell status). Furthermore, these cell properties also differed between field and bottle incubations. To what extent these differences affect phytoplankton dynamics in general, and the ecumenical iron hypothesis (Cullen 1995) in particular, is discussed in more detail below.

Role of iron on phytoplankton biomass

Flow cytometry provides an accurate inventory of the numerical abundance of different size classes of algae in the phytoplankton community. After proper calibration (Fig. 1) even size-class-specific carbon and chl *a* values, and hence also Φ, could be determined. In the case of cell size, the calibration was based on estimating a mean cell diameter applying polycarbonate filters with different pore sizes. The increase in the flow cytometric derived size during the survey corroborated with an increase in mean ESD during the different filtration steps, i.e. cells increased in size and therefore also in carbon content upon iron enrichment. In a similar manner, the flow cytometry derived chl *a* autofluorescence signal and the absolute chemically measured chl *a* content covaried. However, this parameter is also affected by light and macronutrients and not exclusively by iron (Cavender-Bares et al. 1999, and references therein). The correlation of different chl *a* signals in the field confirms a previous finding that used over 100 different species and strains of phytoplankton, grown under optimal conditions (data not shown). Also, under laboratory conditions, a clear correlation between both chl *a* estimates was found (Veldhuis et al. 1997). Only the presence of phycoerythrin in a few species of phytoplankton like *Synechococcus* spp. can result in an overestimation of the chl *a* content of 20 to 30%. This is due to a crossover of the fluorescent signal of this pigment into the red (chlorophyll) channel. This crossover can be compensated for but because of the low abundance of *Synechococcus* spp. the importance of this factor in the present study was almost negligible.

In a previous iron enrichment experiment, a covariation of the chl *a* autofluorescence signal of *Prochlorococcus* and the chl a_2 of this algal species was found, but this relationship was not extended to the rest of the phytoplankton community (Cavender-Bares et al. 1999). In the present study, this relationship was restricted to <20 µm phytoplankton. This size limit corresponded to the (practical) upper size limit of the applied flow cytometer and was nearly identical inside

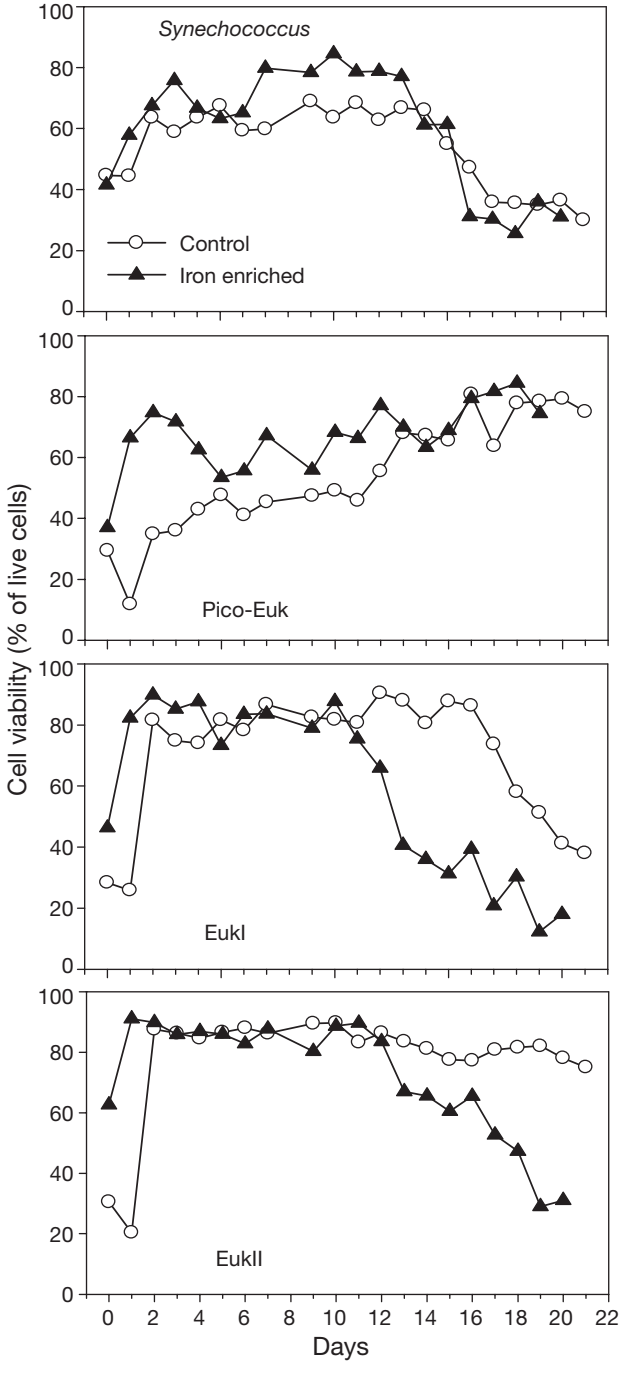

Fig. 10. Cell viability (% of live cells) of 4 different size classes of phytoplankton in iron-enriched water and control bottle

and outside the iron-enriched area (Fig. 1B). The only difference between both regions was the ambient iron concentration, since macronutrient concentrations were high and certainly not limiting phytoplankton growth. We can therefore confidently convert the flow cytometric estimates of chl *a* autofluorescence into absolute chl *a* concentrations of individual cells using the empirical relationship obtained.

The observed increase in algal biomass after iron enrichment was mainly due to an increase in biomass of larger algae (>8 µm) starting from Day 10 onwards. This was approximately 5 d later than reported by Gervais et al. (2002), but they used a phytoplankton fraction ranging from 2 to 20 µm. In this respect, the field observations and bottle incubations showed a similar response. In contrast, changes in the various algal groups <8 µm showed variations in numerical dominance as well as in their carbon and chl *a* content by a factor of 3 or less (cf. Cavender-Bares et al. 1999, DeBaar & Boyd 2000, Gall et al. 2001). These variations were independent of iron concentration and could therefore be a reflection of the patchy spatial distribution of phytoplankton. In more detail, and particularly visible in the bottles, a clear but moderate increase in cell abundance of cells <8 µm occurred in the first week of sampling (Fig. 8). In the second week, cell numbers declined again, resulting in near extinction of *Synechococcus* spp. and pico-Euk in the bottles. The reduction in the standing stock of these 2 phytoplankton populations is most likely caused by enhanced grazing activity of microzooplankton (cf. Landry et al. 2000, Mann & Chisholm 2000). In this respect, the present results align with dynamics of the small phytoplankton as formulated in the ecumenical iron hypothesis by Cullen (1995).

Incubation artifacts

In both the bottle incubation experiments and *in situ*, phytoplankton biomass showed an overall increase in time, but the magnitude of this enhancement differed considerably between these types of experiments. On an areal basis in the field, chl *a* increased by a factor of 1.4 and phytoplankton carbon by a factor of 1.9. In contrast, values of biomass in the incubation bottles reached much higher values (14- to 25-fold for chl *a* and ca. 100-fold for total carbon (Fig. 7). In fact phytoplankton biomass in the bottles was ultimately limited by depletion of macronutrients (Fig. 7). In contrast, the concentration of macronutrients in the field declined only by a few µmol l^{-1} (data not shown). This apparent growth potential of the phytoplankton community to produce dense blooms, even without the amendment of iron (Buma et al. 1991, Timmermans et al. 1998, Olson et al. 2000), is often attributed to so-called 'bottle effects'. Our present experiments also revealed some typical indications of 'bottle effects', like the initial drop of the F_v:F_m, immediately after transfer of the field sample into a bottle. The rapid recovery of the physiological status of the phytoplank-

ton community in the subsequent days is also a typical 'bottle effect' (Figs. 7F & 10). This decline in F_v:F_m was independent of the iron-amendment, but the recovery of the phytoplankton community, 2 d to the initial level, was the same in both bottles. Apparently, this type of physiological response is a general sign of stress, and in the present case not exclusively related to iron depletion (Gervais et al. 2002, Sosik & Olson 2002) or macronutrient limitation (Berges & Falkowski 1998, Young & Beardall 2003). We observed a similar drop in F_v:F_m after transferring phytoplankton cultures into new media (Veldhuis et al. 2001), and also in the field even when incubation containers as large as 1000 l were used (M. Veldhuis unpubl. results).

The containment of phytoplankton also affects the fraction of non-viable cells (those with an impaired cell membrane, Fig. 10). Despite very gentle sampling and careful filling of the bottles, there was a rapid increase in the percentage of live cells. Most likely, the fragile (non-viable) cells were more susceptible to manipulation than the viable fraction, resulting finally in the disintegration of the non-viable cells during the first few days of the incubation. This resulted in a concurrent shift towards a higher percentage of live cells. It has also been observed that non-viable cells show up to 40% reduced (^{14}C-based) primary productivity (Veldhuis et al. 2001). So it seems reasonable to suggest that a lower photosynthetic activity coincides with a reduced F_v:F_m (Berges & Falkowski 1998). The present data showing the coexistence of both viable and non-viable cells of a single population could therefore explain the co-occurrence of cells differing in F_v:F_m observed in some phytoplankton species in the Southern Ocean (Olson et al. 2000). Using the single cell pump-during-probe (PDP) flow cytometry, Olson et al. (2000) observed a bimodal distribution of the F_v:F_m in both *Phaeocystis* sp. and *Corethron* sp. in the same sample. Cells with a low F_v:F_m would therefore belong to the non-viable fraction, whereas cells with a high F_v:F_m would be the healthy (live) part of the population. The overall implication of these differences in the physiological properties, cell viability, and growth potential is that these phytoplankton populations possess a high degree of intraspecific variability. Moreover, changes in the physiological response of a phytoplankton community would not necessary reflect the whole population but could also imply a change in the ratio of viable to non-viable fraction.

A general improvement in the 'health' of a cell ultimately enhances growth rate of the phytoplankton population. A doubling of the proportion of live cells results in an increase in the growth rate by as much as 25% (cf. Veldhuis et al. 2001). In the case of the smallest sized phytoplankton cells (*Synechococcus* spp. and pico-Euk, Fig. 7) this increase in cell abundance was soon followed by a rapid increase in grazing pressure (cf. Landry et al. 2000, Mann & Chisholm 2000). This enhanced grazing rate is also a typical bottle artifact mainly due to the exclusion of larger zooplankton in the bottles normally preying on the smaller grazers (i.e. microzooplankton). With abundant phytoplankton available as prey the microzooplankton will increase rapidly in numbers, thus reducing the cell numbers of the smaller phytoplankton cells.

Changes in the cell viability also explain another 'bottle effect' observed at the end of the incubation experiment. From Day 15 onwards there was a second drop in the percentage of live cells (Fig. 10). This mainly affected the larger sized phytoplankton groups (EukI and EukII) in the iron-enriched bottle. Unlike in the control bottle, macronutrients were depleted in this bottle, resulting in a reduction of the fraction of live cells followed by a decline in the numerical cell abundance. Interestingly, the F_v:F_m ratio in the iron-enriched bottle was far less reduced compared to the control bottle, suggesting that iron partly compensates for the reducing effect of macronutrient limitation on the F_v:F_m.

Control by light

Next to iron, light stress is probably most responsible for the poor physiological condition of the phytoplankton community in the field (Sunda & Huntsman 1997, DeBaar et al. 2005); relief of the light stressor, can result in a major improvement of cell viability and growth. For insight in the specific role of light, Φ is a good indicator, since this ratio provides information on the chl *a* density of the cells. When compared with the temperate and subtropical regions of the Atlantic Ocean, the presently measured values of Φ in the Southern Ocean (Fig. 5D) are at least 2-fold lower than those observed in temperate and subtropical Atlantic waters (Fasham et al. 1985, Li et al. 1992, Carlson et al. 1996, Veldhuis & Kraay 2004). Assuming the same carbon density of a given cell size, this implies that phytoplankton in the Southern Ocean, with exception of *Synechococcus* spp., possesses on average a 2-fold higher chl *a* content per unit of carbon biomass compared with the phytoplankton in the temperate and subtropical region of the North Atlantic. This higher cellular chl *a* density implies a proportional higher demand for iron required for the photosynthetic system. Consequently, iron-limitation in phytoplankton from the Southern Ocean should also be more severe compared to other oceanic basins. During the day, phytoplankton cells experience continuous changes in light conditions, mainly due to strong daily vertical mixing of the upper water column. As a result, the chl *a* density will be an average re-

sponse to this varying light climate. The absence of a chl *a* density gradient, at least in the euphotic zone, suggests a high degree of similarity of the phytoplankton community in the mixed layer. Whereas most of this daily mixing was within the euphotic zone, there was also a deep vertical mixing with a frequency of 3 to 4 d (DeBaar et al. 2005). The overall effect of this more severe physical mixing process was that the euphotic zone contained (towards the end of the field experiment) only 30% of the total phytoplankton biomass. Phytoplankton cells will therefore also experience, along with the continuously changing light conditions in the upper water layers, a prolonged nearly dark period when they are below the euphotic zone. Furthermore, photosynthetic activity, which compensates for the induced changes at the cellular level due to the highly variable light dynamics, is also reduced since active primary production is restricted to the (upper) part of the euphotic zone only (Gervais et al. 2002). In a recent synthesis of 8 iron enrichment experiments, DeBaar et al. (2005) concluded that the wind mixed layer, and associated changes in the light condition, classified the EisenEx iron enrichment experiment as one with the lowest overall increase in phytoplankton biomass upon iron repletion in terms of biomass increase per cubic metre or per square metre of surface. This (vertical) physical dilution process, however, is largely compensated for if the whole iron-enriched area is taken into account (ca. 950 km^2).

In view of the present results, it seems that growth of the smaller sized phytoplankton community (<20 µm) was negatively affected by a combination of iron-limitation and the continuously changing light conditions. Upon relief of the light stressor, i.e. during the bottle experiments, the physiology of cells in all size classes improved significantly, resulting in accelerated growth and biomass production. Similar to the growth response of the phytoplankton fraction >20 µm (Gervais et al. 2002), growth of the larger sized cells in our study (8 to 20 µm) was particularly triggered by iron. Despite ample nutrients and the apparent high affinity for iron, the prevailing dynamics in the light conditions in the field prevented the small algae from improving their (poor) physiological condition. Recently, a comparable type of response was observed, where, under nutrient-replete and light-favorable conditions, the cell physiology of smaller-sized phytoplankton was reduced compared to the larger cells (Cermeño et al. 2005). In view of our observations, the ecumenical hypothesis (Cullen 1995) should also include a physical/optical dynamic module, next to the specific role of microzooplankton. This second controlling factor increases in importance with increasing (wind induced) vertical water mixing and seems to be affecting in particular the smallest algae in the phytoplankton community.

Acknowledgements. The authors thank the captain and crew of RV 'Polarstern' as well as V. Smetacek and U. Bathmann for the organization of the EisenEx cruise. U. Riebesell and colleagues are acknowledged for providing chl *a* data, P. Croot for iron data and V. Strass and colleagues for the physical data. We also thank 2 anonymous reviewers and M. Sieracki for their helpful comments. This research was supported by the Netherlands AntArctic Program (NAAP) grant Fe *in-situ* (to K.R.T.).

LITERATURE CITED

Berges JA, Falkowski PG (1998) Physiological stress and cell death in marine phytoplankton: induction of proteases in response to nitrogen and light limitation. Limnol Oceanogr 43:129–135

Blain S, Guieu C, Claustre H, Leblanc K, Moutin T, Queguiner B, Ras J, Sarthou G (2004) Availability of iron and major nutrients for phytoplankton in the north-east Atlantic Ocean. Limnol Oceanogr 49:2095–2104

Boyd PW, Abraham ER (2001) Iron-mediated changes in phytoplankton during photosynthetic competence during SOIREE. Deep-Sea Res I 48:2529–2550

Boyd PW, Watson AJ, Law CS, Abraham ER and 31 others (2000) A mesoscale phytoplankton bloom in the polar Southern Ocean stimulated by iron fertilization. Nature 407:695–702

Boyd PW, Law CS, Wong CS, Nojiri Y and 34 others (2004) The decline and fate of an iron-induced subarctic phytoplankton bloom. Nature 428:549–553

Bucciarelli E, Blain S, Tréguer P (2001) Iron and manganese in the wake of the Kerguelen Islands (Southern Ocean). Mar Chem 73:21–36

Buma AGJ, DeBaar HJW, Nolting RF, van Bennekom AJ (1991) Metal enrichment experiments in the Weddell-Scotia Seas: effects of iron and manganese on various plankton communities. Limnol Oceanogr 36:1865–1878

Carlson CA, Ducklow HW, Sleeter TD (1996) Stocks and dynamics of bacterioplankton in the northwestern Sargasso Sea. Deep-Sea Res II 43:491–515

Casotti R, Mazza C, Brunet C, Vantrepotte V, Ianora A, Miralto A (2005) Growth inhibition and toxicity of the diatom aldehyde 2-trans-4trans decadienal on *Thalassiosira weissflogii* (Bacillariophyceae). J Phycol 41:7–20

Cavender-Bares KK, Mann EL, Chisholm SW, Ondrusek ME, Bidigare RR (1999) Differential response of equatorial Pacific phytoplankton to iron fertilization. Limnol Oceanogr 44:237–246

Cavender-Bares KK, Rinaldo A, Chisholm SW (2001) Microbial size spectra from natural and nutrient enriched ecosystems. Limnol Oceanogr 46:778–789

Cermeño P, Estévez-Blanco P, Marañón E, Fernández E (2005) Maximum photosynthetic efficiency of size-fractionated phytoplankton assessed by ^{14}C uptake and fast repetition rate fluorometry. Limnol Oceanogr 50: 1438–1446

Croot PL, Laan P, Nishioka J, Strass V and 6 others (2005) Spatial and temporal distribution of Fe(II) and H_2O_2 during EisenEx, an open ocean mesoscale iron enrichment. Mar Chem 95:65–88

Cullen JJ (1995) Status of the iron hypothesis after the Open Ocean Enrichment Experiment. Limnol Oceanogr 40: 1336–1343

Cullen JJ, Davis RF (2003) The blank can make a big difference in oceanographic measurements. Limnol Oceanogr Bull 12:29–35

DeBaar HJW, Boyd PM (2000) The role of iron in plankton ecology and carbon dioxide transfer of the global oceans. In: Hanson RB, Ducklow HW, Fields JG (eds) The dynamic ocean carbon cycle: a midterm synthesis of the Joint Global Ocean Flux Study. International Geosphere Biosphere Programme Book Series, Vol 5. Cambridge University Press, Cambridge, p 61–140

DeBaar HJW, DeJong JTM, Bakker DCE, Löscher BM, Veth C, Bathmann U, Smetacek V (1995) Importance of iron for phytoplankton spring blooms and CO_2 drawdown in the Southern Ocean. Nature 373:412–415

DeBaar HJW, Boyd PW, Coale KH, Landry MR and 30 others (2005) Synthesis of iron fertilization experiments: from the iron age in the age of enlightenment. J Geophys Res 110:doi:10.1029/2004JC002601, 002005

DeJong JTM, den Das J, Bathmann U, Stoll MHC, Kattner G, Nolting RF, DeBaar HJW (1998) Dissolved iron at subnanomolar levels in the Southern Ocean as determined by ship-board analysis. Anal Chim Acta 377:113–124

Dubelaar GBJ, Jonker RR (2000) Flow cytometry as a tool for the study of phytoplankton. Sci Mar 64:135–156

Fasham MJR, Platt T, Irwin B, Jones K (1985) Factors affecting the spatial pattern of the deep chlorophyll maximum in the region of the Azores front. Prog Oceanogr 14:129–165

Gall MP, Boyd PM, Hall J, Safi KA, Chang H (2001) Phytoplankton processes. Part 1. Community structure during the Southern Ocean Iron RElease Experiment (SOIREE). Deep-Sea Res II 48:2551–2570

Gervais F, Riebesell U, Gorbunov MY (2002) Changes in primary productivity and chlorophyll *a* in response to iron fertilization in the Southern Polar Frontal Zone. Limnol Oceanogr 47:1324–1335

Gorbunov MY, Kolber Z, Falkowski PG (1999) Measuring photosynthetic parameters in individual cells by Fast Repetition Rate fluorometry. Photosynth Res 62:141–153

Kolber ZS, Barber RT, Coale KH, Fitzwater SE, Greene RM, Johnson KS, Lindley S, Falkowski PG (1994) Iron limitation of phytoplankton photosynthesis in the equatorial Pacific Ocean. Nature 371:145–149

Landry MR, Ondrusek ME, Tanner SJ, Brown SL, Constantinou J, Bidigare RR, Coale KH, Fitzwater S (2000) Biological response to iron fertilization in the eastern equatorial Pacific (IronEx II). I. Microplankton community abundances and biomass. Mar Ecol Prog Ser 201:27–42

Li WKW, Dickie PM, Irwin BD, Wood AM (1992) Biomass of bacteria, cyanobacteria, prochlorophytes and photosynthetic eukaryotes in the Sargasso Sea. Deep-Sea Res I 39: 501–519

Mann EL, Chisholm SW (2000) Iron limits the cell division rate of *Prochlorococcus* in the eastern equatorial Pacific. Limnol Oceanogr 45:1067–1076

Martin JH, Fitzwater SE (1988) Iron deficiency limits phytoplankton growth in the northeast Pacific subarctic. Nature 331:341–343

Olson RJ, Sosik HM, Chekalyuk AM, Shalapyonok A (2000) Effects of iron enrichment on phytoplankton in the Southern Ocean during late summer: active fluorescence and flow cytometric analyses. Deep-Sea Res II 47:3181–3200

Schreiber U, Neubauer C, Schliwa U (1993) PAM fluorometer based on medium-frequency pulsed Xe-flash measuring light: a highly sensitive new tool in basic and applied photosynthesis. Photosynth Res 36:65–72

Sosik HM, Olson RJ (2002) Phytoplankton and iron limitation of photosynthetic efficiency in the Southern Ocean during late summer. Deep-Sea Res I 49:1195–1216

Strass V, Leach H, Cisewski B, Gonzalez S, Post J, Duarte VD, Trumm F (2001) The physical setting of the Southern Ocean fertilization experiment. Ber Polar Meeresforsch 400:94–130

Sunda WG, Huntsman SA (1995) Iron uptake and growth limitation in oceanic and coastal phytoplankton. Mar Chem 50:189–206

Sunda WG, Huntsman SA (1997) Interrelated influence of iron, light and cell size on growth of marine phytoplankton. Nature 390:389–392

Timmermans KT, van Leeuwe MA, de Jong JTM, McKay RML and 6 others (1998) Iron stress in the Pacific region of the Southern Ocean: evidence from enrichment bioassays. Mar Ecol Prog Ser 166:27–41

Timmermans KR, Gerringa LJA, DeBaar HJW, van der Wagt B, Veldhuis MJW, DeJong JTM, Croot PL, Boye M (2001) Growth rates of large and small Southern Ocean diatoms in relation to availability of iron in natural seawater. Limnol Oceanogr 46:260–266

Timmermans KR, van der Wagt B, DeBaar HJW (2004) Growth rates, half-saturation constants, and silicate, nitrate, and phosphate depletion of four large, open-ocean diatoms from the Southern Ocean. Limnol Oceanogr 49: 2141–2151

Tsuda A, Takeda S, Saito H, Nishioka J and 22 others (2003) A mesoscale iron enrichment in the western Subarctic Pacific induces a large centric diatom bloom. Science 300: 958–961

Veldhuis MJW, Kraay GW (2000) Application of flow cytometry in marine phytoplankton research: current applications and future perspectives. Sci Mar 64:121–134

Veldhuis MJW, Kraay GW (2004) Phytoplankton in the subtropical Atlantic Ocean: towards a better assessment of biomass and composition. Deep-Sea Res I 51:507–530

Veldhuis MJW, Cucci TL, Sieracki ME (1997) Cellular DNA content of marine phytoplankton using two new fluorochromes: taxonomic and ecological implications. J Phycol 33:527–541

Veldhuis MJW, Kraay GW, Timmermans KR (2001) Cell death in phytoplankton: correlation between changes in membrane permeability, photosynthetic activity, pigmentation and growth. Eur J Phycol 36:167–177

Veldhuis MJW, Brussaard CPD, Noordeloos AAM (2005a) Living in a *Phaeocystis* colony; a way to be a successful algal species. Harmful Algae 4:841–858

Veldhuis MJW, Timmermans KR, Croot P, van der Wagt B (2005b) Picophytoplankton; a comparative study of their biochemical composition and photosynthetic properties. J Sea Res 53:7–24

Verity P, Robertson CY, Tronzo CR, Nelson JR, Sieracki ME (1992) Relationships between cell volume and the carbon and nitrogen content of marine photosynthetic nanoplankton. Limnol Oceanogr 37:1434–1446

Watson A, Messias MJ, Goldson L, Skjelvan I, Nightingale P, Liddicoat M (2001) SF6 measurements on EisenEx. Ber Polar Meeresforsch 400:76–79

Young EB, Beardall J (2003) Photosynthetic function in *Dunaliella tetriolecta* (chlorophyta) during a nitrogen starvation and recovery cycle. J Phycol 39:897–905

Editorial responsibility: Josep Gasol, Barcelona, Spain

Submitted: February 13, 2006; Accepted: October 19, 2006
Proofs received from author(s): April 26, 2007